

This article was downloaded by: [Chongqing University]

On: 14 February 2014, At: 13:26

Publisher: Taylor & Francis

Informa Ltd Registered in England and Wales Registered Number: 1072954 Registered office: Mortimer House, 37-41 Mortimer Street, London W1T 3JH, UK



Journal of Coordination Chemistry

Publication details, including instructions for authors and subscription information:

<http://www.tandfonline.com/loi/gcoo20>

Determination of the stability constants of $\text{Pb}-(\text{DIPSO})_x-(\text{OH})_y$ and $\text{Pb}-(\text{AMPSO})_x-(\text{OH})_y$ systems

Maxime Eliat-Eliat^{ab}, Isabel S.S. Pinto^a, Georgina M.S. Alves^a, Victor Ollé^{ab} & Helena M.V.M. Soares^a

^a REQUIMTE, Department of Chemical Engineering, University of Porto, Porto, Portugal

^b Department of Biochemistry-Microbiology, Industrial Engineering, KaHo St. Lieven, Gent, Belgium

Accepted author version posted online: 13 Sep 2013. Published online: 06 Nov 2013.

To cite this article: Maxime Eliat-Eliat, Isabel S.S. Pinto, Georgina M.S. Alves, Victor Ollé & Helena M.V.M. Soares (2013) Determination of the stability constants of $\text{Pb}-(\text{DIPSO})_x-(\text{OH})_y$ and $\text{Pb}-(\text{AMPSO})_x-(\text{OH})_y$ systems, *Journal of Coordination Chemistry*, 66:20, 3544-3560, DOI: [10.1080/00958972.2013.842641](https://doi.org/10.1080/00958972.2013.842641)

To link to this article: <http://dx.doi.org/10.1080/00958972.2013.842641>

PLEASE SCROLL DOWN FOR ARTICLE

Taylor & Francis makes every effort to ensure the accuracy of all the information (the "Content") contained in the publications on our platform. However, Taylor & Francis, our agents, and our licensors make no representations or warranties whatsoever as to the accuracy, completeness, or suitability for any purpose of the Content. Any opinions and views expressed in this publication are the opinions and views of the authors, and are not the views of or endorsed by Taylor & Francis. The accuracy of the Content should not be relied upon and should be independently verified with primary sources of information. Taylor and Francis shall not be liable for any losses, actions, claims, proceedings, demands, costs, expenses, damages, and other liabilities whatsoever or howsoever caused arising directly or indirectly in connection with, in relation to or arising out of the use of the Content.

This article may be used for research, teaching, and private study purposes. Any substantial or systematic reproduction, redistribution, reselling, loan, sub-licensing, systematic supply, or distribution in any form to anyone is expressly forbidden. Terms &

Conditions of access and use can be found at <http://www.tandfonline.com/page/terms-and-conditions>

Determination of the stability constants of Pb–(DIPSO)_x–(OH)_y and Pb–(AMPSO)_x–(OH)_y systems

MAXIME ELIAT-ELIAT^{†‡}, ISABEL S.S. PINTO[†], GEORGINA M.S. ALVES[†],
VICTOR OLLE^{†‡} and HELENA M.V.M. SOARES^{*†}

[†]REQUIMTE, Department of Chemical Engineering, University of Porto, Porto, Portugal

[‡]Department of Biochemistry-Microbiology, Industrial Engineering, KaHo St. Lieven, Gent, Belgium

(Received 6 May 2013; accepted 7 August 2013)

In this work, complexation between lead ion and the ligands 3-[N,N-bis(2-hydroxyethyl)amino]-2-hydroxypropanesulfonic acid (DIPSO) and N-(1,1-dimethyl-2-hydroxyethyl)-3-amino-2-hydroxypropanesulfonic acid (AMPSO), which are commercial pH buffers, is presented. Both ligands form complexes with lead in their pH buffer range (between pH 6.5 and 8.5 for DIPSO and between pH 8.0 and 9.0 for AMPSO). The final models and the overall stability constants, which are reported here, were determined by direct current polarography and glass electrode potentiometry [only for the Pb–(DIPSO)_x–(OH)_y system] at 25.0 °C and 0.1 M KNO₃ ionic strength. For the Pb–(DIPSO)_x–(OH)_y system, the proposed final model contains PbL, PbL₂, PbL₂(OH), and PbL₂(OH)₂ with stability constants, as log β, of 3.4 ± 0.1, 6.35 ± 0.15, 12.8 ± 0.2, and 18.0 ± 0.3, respectively. For the Pb–(AMPSO)_x–(OH)_y system, the species observed are PbL, PbL(OH), and PbL(OH)₂ with stability constants, as log β, of 2.9 ± 0.5, 9.4 ± 0.1, and 14.5 ± 0.2, respectively. For AMPSO, the possible adsorption of the ligand at the mercury electrode surface was evaluated by alternating current polarography through calculation of the capacitance of the double layer.

Keywords: DIPSO; AMPSO; Stability constants; Lead; Electrochemical techniques

1. Introduction

The concentration of hydrogen ions is of importance in biological and chemical systems. Hydrogen ion concentrations have important implications in cell metabolism by affecting the rates of enzymatic reactions and the stability of biological molecules. For example, maintenance of an appropriate pH range in tissue culture media is critical to the growth and viability of all cultured cells. The efficiency of many chemical separations and the rate of many chemical reactions are controlled by the pH of the solution. Buffers can also be used to control the rates and yields in organic synthesis. The hydrogen ion concentration is also an important parameter to be controlled in electrophoresis, chromatography, and immunoassays. Uncontrolled pH can result in unsuccessful immunoassays, since the required protein–protein interactions cannot occur efficiently outside the range of physiological pH. When metal speciation studies are carried out in natural waters, model solutions, or culture media for organisms, it is usually desirable to maintain a constant pH of the solution. From all the

*Corresponding author. Email: hsoares@fe.up.pt

examples stated previously, selection of an appropriate buffer to keep the pH of the solution constant, while other components in the reaction mixture are varied, is crucial.

In 1966, Good *et al.* described several biological buffers which are compatible with most common physiological media [1]. Most of these buffers are zwitterionic, containing both positive and negative ionizable groups provided by secondary or tertiary amines and sulfonic and carboxylic acid groups. Among these biological buffers, 3-[*N,N*-bis(2-hydroxyethyl)amino]-2-hydroxypropanesulfonic acid (DIPSO) and 2-hydroxy-3-[(2-hydroxy-1,1-dimethylethyl)amino]propane-1-sulfonic acid (AMPPO) are the two examples of pH buffers, commercialized by various suppliers, and widely used in several biological [2–4], biochemical [5–7], chemical [8–12], and environmental [13] studies. The pH buffer range is between pH 6.5 and 8.5 for DIPSO and between pH 8.0 and 10.0 for AMPPO.

DIPSO and AMPPO possess tertiary and secondary amines, respectively, and also β -alcohol groups, which can all potentially coordinate to metals. In fact, it has been shown that these ligands complex with copper [14, 15], cadmium, and zinc [16, 17] in solution. Thus, it is expected that DIPSO or AMPPO also complexes lead. However, as far as we know, no reports regarding studies of the interaction between DIPSO or AMPPO and lead are described in literature.

Therefore, this work evaluates the complexation between lead and these two ligands. The overall stability constants were determined by direct current polarography (DCP) and glass electrode potentiometry (GEP; only for lead-DIPSO system), at fixed total ligand to total lead concentration ($[L_T]:[Pb_T]$) ratios and various pH values at 25.0 °C and 0.1 M KNO_3 ionic strength. Alternating current polarography (ACP) was also run, in the absence of lead ion, for evaluating the adsorption of AMPPO at the surface of the working mercury electrode.

2. Experimental

2.1. Materials and reagents

AMPPO (99.1%) and DIPSO (99%) were purchased from Sigma-Aldrich (St. Louis, Missouri, USA) and used as received. The standard lead solution, 9.6×10^{-3} M, was purchased from Merck.

A stock solution of 0.1 M KOH was standardized against potassium hydrogen phthalate by potentiometric titration as previously described [14]. A stock solution of 0.1 M nitric acid was standardized potentiometrically against the standardized solution of potassium hydroxide.

A detailed description of the remaining reagents and experimental conditions of standardization were reported previously [14].

2.2. Apparatus

All measurements reported in this work were performed on solutions adjusted to ionic strength 0.1 M KNO_3 in a Metrohm (Herisau, Switzerland) jacketed glass vessel, equipped with a magnetic stirrer, and thermostatted at 25.0 ± 0.1 °C using a water bath.

2.2.1. Polarography. Polarographic measurements were performed using a Model 663 VA stand (Metrohm) equipped with a multimode electrode (Metrohm, Model 6.1246.020), as a

working electrode, used in the dropping mercury electrode mode. Silver/silver chloride (3 M KCl) and glassy carbon were used as reference and counterelectrodes, respectively (both from Metrohm). The VA stand was attached to a microAutolab or to a potentiostat–galvanostat model PGSTAT12/30/302, both from Metrohm Autolab (Utrecht, the Netherlands), driven by GPES 4.9 software system controlled by a personal computer. A drop time of 2 s and a step potential of 4 mV were used.

The pH measurements were conducted with a GLP 22 pH meter Crison (Barcelona, Spain) with a sensitivity of ± 0.1 mV (± 0.001 pH units), with a silver/silver chloride reference electrode (Metrohm) and a glass electrode (Metrohm).

2.2.2. Potentiometry. Potentiometric titrations were performed with a PC-controlled system assembled with a Crison MicropH 2002 meter, a Crison MicroBU 2030 micro burette, a Philips GAH 110 glass electrode, and an Orion 90-02-00 (double junction) reference electrode with the outer chamber filled with 0.1 M KNO₃. Automatic acquisition of data was done using a homemade program, COPOTISY.

2.3. Procedure

2.3.1. Calibration of the glass electrode. Calibration of the glass electrode (measurements of pH as $-\log_{10}[\text{H}^+]$) was accomplished by potentiometric titration of HNO₃ with KOH (both standardized solutions). From this potentiometric titration, the E° and the response slope were established, and used to calculate the pH during polarographic and potentiometric titrations.

2.3.2. Alternating current polarography. ACP polarograms were run in the absence of lead to evaluate the adsorption of AMPSO on the surface of the mercury working electrode. All the ACP experiments were performed in 20 mL 0.1 M KNO₃ solution. Scans were performed in 0.1 M KNO₃, which was used as reference, and two concentrations (5.0×10^{-4} and 4.8×10^{-2} M) of AMPSO at two values of pH, $pK_a - 2$ (pH 7) and $pK_a + 2$ (pH 11). Before each scan, the solution was purged using N₂. Scans were performed at two different phase angles: 0° and 90°. For each condition tested, at least two scans that are in agreement were taken. The following experimental conditions were used: dropping time 0.21 s, frequency 75 Hz, step potential 5 mV and amplitude 5 mV.

2.3.3. Direct current polarography. The study of the electrochemical behavior of the Pb-(Ligand)_x-(OH)_y systems was performed by DCP. The procedure used to run the polarographic titrations was described previously [18].

For the Pb-(DIPSO)_x-(OH)_y system, one [L_T]:[Pb_T] ratio, 198, was used in two independent experiments with [Pb_T] of 3.0×10^{-5} and 1.9×10^{-5} M, respectively. The scanned pH range varied between 3 and 11. For each experiment, about 52 and 79 points were obtained, respectively. For the Pb-(AMPSO)_x-(OH)_y system, [L_T]:[Pb_T] ratios of 205 with [Pb_T] = 5.1×10^{-5} M, 402, 450, and 490 (two experiments) with [Pb_T] = 4.0×10^{-5} M, were used. The scanned pH range varied between 3.4 and 11.8. About 65, 48, 36, and 43 points were obtained for each ratio, respectively.

2.3.4. Glass electrode potentiometry. For studying potentiometrically the $\text{Pb}-(\text{DIPSO})_x-(\text{OH})_y$ system, $[\text{L}_T]:[\text{Pb}_T]$ ratio of 6.3 and 10.4 with $[\text{Pb}_T] = 9.65 \times 10^{-4} \text{ M}$ was performed. Monotonic additions ($8 \times 10^{-3} \text{ mL}$) of standardized 0.1 M KNO_3 were done.

2.4. Data treatment

2.4.1. ACP data. For each experimental condition tested (background electrolyte solution or solutions of AMPSO at different concentrations and pH values), the variation of the capacitance as a function of the potential was calculated. Calculation of the capacitance-potential curves was done from the resulting current intensities, recorded by ACP, using two phase angles lagged by $\pi/2$ radians. From the impedance measurement data, the value of the capacitance (C) was calculated using equation (1):

$$C = \frac{-1}{Z'' \times 2 \times \pi \times f} \quad (1)$$

where Z'' is the imaginary component of impedance and f the frequency (for further details, see reference [19]).

2.4.2. DCP and GEP data. For polarographic data, simulation and optimization procedures were performed using the Cukrowski method [20, 21]. This method uses mass-balance equations written for a labile (on the polarographic time scale) and reversible metal–ligand system studied at a fixed $[\text{L}_T]:[\text{M}_T]$ ratio and varied pH. Refinement operations are based on comparative analysis of the experimental (ECFC, which is based on the shift in peak potential and decrease in polarographic peak height caused by formation of metal complexes) and calculated complex-formation curves (CCFC, which is based on the free metal ion concentration calculated from mass-balance equations written for the assumed metal–ligand model). During the iterative operation, values of refined stability constants are varied. The refinement operation is completed when the CCFC better fits the ECFC.

The simulation and optimization procedures of potentiometric data were done using the Equilibrium Simulation for Titration Analysis program [22, 23]. The refinement operations used in potentiometry involve solving mass-balance equations, including the equation for

Table 1. Dissociation constant for water, protonation constant for AMPSO and DIPSO, and overall stability constants for $\text{Pb}_x(\text{OH})_y$ complexes with OH^- at 25°C .

	Equilibrium	Log β	μ	Refs.
Water	$\text{H}^+ + \text{OH}^- \rightleftharpoons \text{H}_2\text{O}$	13.78	0.1	[24]
AMPSO	$\text{L}^- + \text{H}^+ \rightleftharpoons \text{HL}$	9.05	0.1	[25]
DIPSO	$\text{L}^- + \text{H}^+ \rightleftharpoons \text{HL}$	7.47	0.1	[15]
Lead	$\text{Pb}^{2+} + \text{OH}^- \rightleftharpoons \text{Pb}(\text{OH})^+$	5.9	0.1	[24]
	$2\text{Pb}^{2+} + \text{OH}^- \rightleftharpoons \text{Pb}_2(\text{OH})^{3+}$	7.0	1.0	[24]
	$\text{Pb}^{2+} + 2\text{OH}^- \rightleftharpoons \text{Pb}(\text{OH})_2$	10.4	0.3	[26]
	$\text{Pb}^{2+} + 3\text{OH}^- \rightleftharpoons \text{Pb}(\text{OH})_3^-$	13.3	0.3	[26]
	$3\text{Pb}^{2+} + 4\text{OH}^- \rightleftharpoons \text{Pb}_3(\text{OH})_4^{2+}$	31.4	0.1	[26]
	$4\text{Pb}^{2+} + 4\text{OH}^- \rightleftharpoons \text{Pb}_4(\text{OH})_4^{4+}$	34.9	0.1	[26]
	$6\text{Pb}^{2+} + 8\text{OH}^- \rightleftharpoons \text{Pb}_6(\text{OH})_8^{4+}$	67.1	0.1	[26]
	$\text{Pb}(\text{OH})_2(\text{s}) \rightleftharpoons \text{Pb}^{2+} + 2\text{OH}^-$	-16.8	0.0	[27]

total proton concentration, in such a way that the computed free proton concentration, when used by the equation describing the response of the calibrated glass electrode, reproduces the experimentally recorded potential of the glass electrode as accurately as possible.

During refinement of the overall stability constants for both systems, the water dissociation constant [24] and ligand [15, 25] protonation constants, as well as all known stability constants for $\text{Pb}_x(\text{OH})_y$ species [24, 26], were kept fixed (table 1).

3. Results and discussion

3.1. Adsorption and reversibility studies

For accurate determination of stability constants by polarographic techniques, concentration of the ligand at the mercury surface electrode should be the same as in the bulk; this means that no appreciable adsorption of the ligand at the mercury surface electrode should occur.

In a previous study [15], we have demonstrated that up to 1.2×10^{-2} M DIPSO, no significant adsorption of the ligand occurred at the mercury surface electrode. So, in this work, concentrations of DIPSO lower than 1.2×10^{-2} M were used in the DCP experiments.

Assessment of adsorption of AMPSO at the DME was performed by calculating the capacitance-potential curves for two different concentrations of AMPSO (5.0×10^{-4} and 4.8×10^{-2} M) at a $\text{pH} = \text{p}K_a \pm 2$ (at $\text{pH} = \text{p}K_a - 2$, the ligand is totally protonated, HL; at $\text{pH} = \text{p}K_a + 2$, the ligand is totally deprotonated, L⁻), as well as for the background electrolyte (figure 1). For the lowest ligand concentration, the variation of the capacitance was similar to the one recorded for the electrolyte in all ranges of potential for both pH values; these results show that no adsorption of AMPSO occurs at the mercury electrode. Comparing the capacitance-potential curves recorded in the presence of the higher ligand concentration (4.8×10^{-2} M) and in the presence of the background electrolyte, we see a very small difference mainly in the potential range between -0.2 and -0.6 V (figure 1). From these results, for AMPSO concentrations up to 4.8×10^{-2} M, the adsorption is negligible and thus, we can safely use the ligand up to this concentration.

The determination of the overall stability constants by voltammetric techniques using the Cukrowski method [20, 21] presupposes that besides the absence of adsorption phenomena

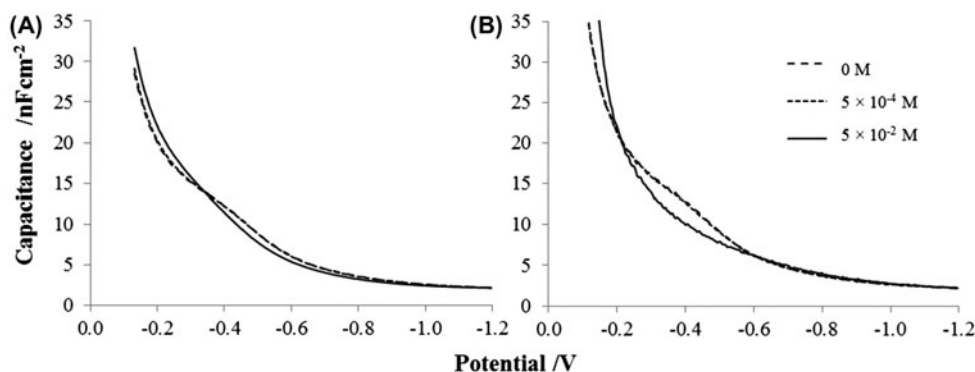


Figure 1. Capacitance – potential curves for AMPSO at pH 7 (A) and pH 11 (B).

at the electrode, the system is also electrochemically reversible. For DCP, the reversibility of the metal electrochemical reaction can be quantified in terms of the recorded wave steepness [28]. For the $\text{Pb}-(\text{DIPSO})_x-(\text{OH})_y$ system, the steepness of the recorded waves varied between 1.0 and 0.88 in the pH range 3.0 and 11.0 for both titrations performed. For the $\text{Pb}-(\text{AMP SO})_x-(\text{OH})_y$ system, the steepness of the recorded waves varied between 1.0 and 0.93 in the pH range 3.4 and 11.8 for all titrations performed. These results show a slight increase of the irreversibility of the reduction process for higher pH. In order to use the collected data, and since the limiting diffusion current does not depend on the degree of the reversibility of the electrochemical process, a correction of the irreversibility already used successfully in another system was applied [14].

3.2. Modeling and determination of the overall stability constants for Pb–ligand systems

3.2.1. Pb–DIPSO system. First, two independent DCP titrations, performed at $[\text{L}_T]:[\text{Pb}_T]$ ratio 198 with $[\text{Pb}_T]$ of 3.0×10^{-5} and 1.9×10^{-5} M, were carried out. Although two independent experiments were performed, the following graphic analysis will be presented for just one, as an example. In figure 2(A), the variation of the half-wave potential ($E_{1/2}$) as a function of pH is presented for $[\text{L}_T]:[\text{Pb}_T] = 198$, $[\text{Pb}_T] = 3.0 \times 10^{-5}$ M, for Pb–DIPSO system. The protonation constant and the different forms of the ligand are also indicated in

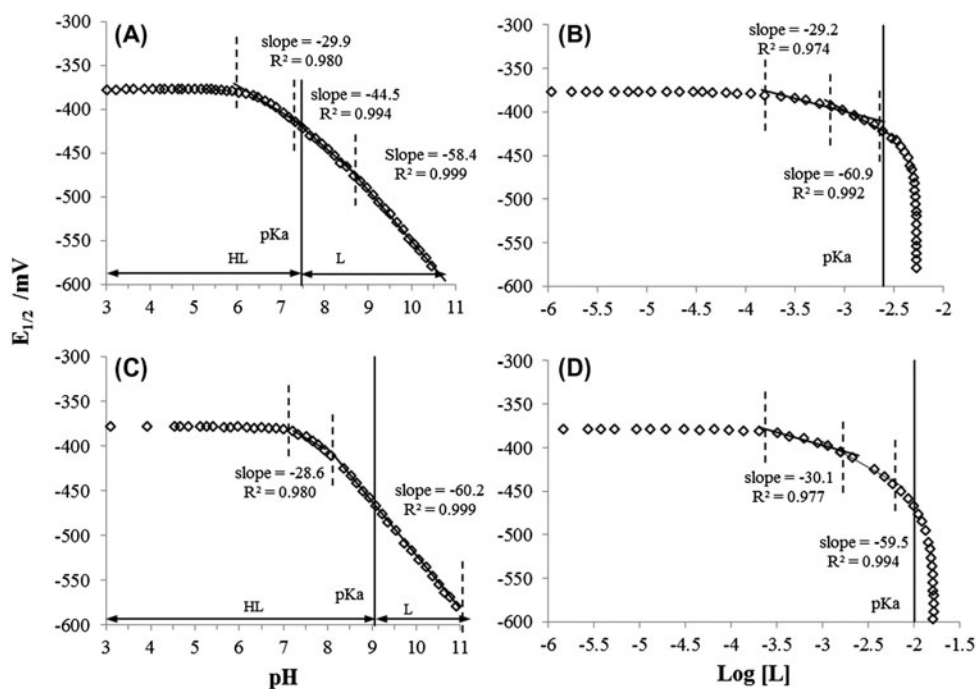
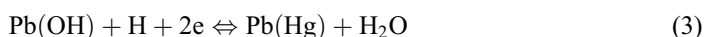


Figure 2. Half-wave potential shift as a function of pH (A, C) and the free ligand concentration (B, D), recorded by DCP, for $\text{Pb}-(\text{DIPSO})_x-(\text{OH})_y$ and $\text{Pb}-(\text{AMP SO})_x-(\text{OH})_y$ systems. (A, B) $\text{Pb}-(\text{DIPSO})_x-(\text{OH})_y$ system: $[\text{L}_T]:[\text{Pb}_T] = 198$ with $[\text{Pb}_T] = 3.0 \times 10^{-5}$ M. (C, D) $\text{Pb}-(\text{AMP SO})_x-(\text{OH})_y$ system: $[\text{L}_T]:[\text{Pb}_T] = 490$, $[\text{Pb}_T] = 4.0 \times 10^{-5}$ M.

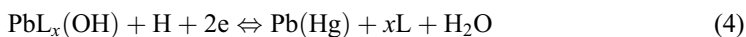
the figure. The analysis and interpretation of the variation of the slopes predict which $\text{PbL}_x(\text{OH})_y$ species ($x = 1$ or 2 and $y = 0, 1$ or 2) are present in the solution.

The analysis of figure 2(A) shows that the half-wave potential became more cathodic when the pH increases; this behavior showed that the Pb–DIPSO system behaved as labile on the polarographic time. From the experimental points, four distinct regions can be drawn. The first region shows that no significant complexation occurs up to pH 6; for higher pH, which corresponds to the pH range where the ligand starts to be deprotonated, a significant complexation occurs and different slopes can be identified. From pH 6 to 7.4, a slope of about 30 mV/pH was identified; this slope indicates formation of PbL and/or $\text{Pb}(\text{OH})$ in solution. According to the reduction reactions at the DME electrode involving one proton (charges will be omitted, for the sake of simplicity):

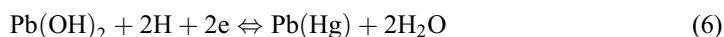
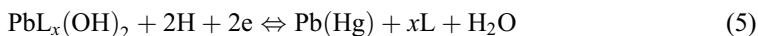


A slope of 29.5 mV/pH should be obtained for both reactions.

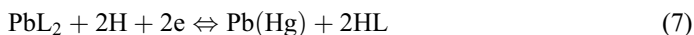
Between pH 7.4 and 8.6, a slope of 44 mV/pH was obtained. In this pH range, which is above the $\text{p}K_a$ value, the ligand is mainly in the deprotonated form; so, the reduction reaction of $\text{PbL}_x(\text{OH})$, at the DME electrode involving one proton, results in a theoretical slope of 29.5 mV/pH:



On the other hand, reduction reactions of $\text{PbL}_x(\text{OH})_2$ and $\text{Pb}(\text{OH})_2$ at the DME electrode involve two protons, resulting in a theoretical slope of 59 mV/pH:



Precipitation was not observed, indicating that lead hydroxide can be excluded as a major species; therefore, it is more likely that lead is complexed by the ligand in this pH range. The fact that a slope of 44 mV/pH was obtained can be explained by the formation of a mixture of $\text{PbL}_x(\text{OH})$ and $\text{PbL}_x(\text{OH})_2$ in the pH range considered. However, although the ligand is mainly in the deprotonated form between pH 7.4 and 8.6, some amount of HL still exists. Thus, the increase in the slope can also be due to formation of PbL_2 according to the following electrochemical reduction reactions at the DME:



These electrochemical reactions generate theoretical slopes of 59 and 0 mV/pH since two or zero protons are involved, respectively. Above pH 8.6, a slope of about 59 mV/pH can be drawn, which suggests the formation of $\text{PbL}_x(\text{OH})_2$ (see equation (5) above).

Analysis of the half-wave potential as a function of $\log[\text{L}]$ (figure 2(B)) confirmed the formation of PbL in solution, since a slope of 29 mV/ $\log[\text{L}]$ could be drawn. In addition,

the points between $\log[L] -2.9$ and -2.6 , relative to the pH range 7.1–7.5, clearly suggest the formation of PbL_2 with a slope of 61 mV/ $\log[L]$, close to the theoretical Nernst slope (59 mV/ $\log[L]$).

From the analysis described above, the modeling and refinement operations of the stability constants for the Pb-DIPSO system were performed considering two possible models:

- (I) $PbL, PbL(OH), PbL(OH)_2$
- (II) $PbL, PbL_2, PbL_2(OH), PbL_2(OH)_2$

Assuming the two models described above, ECFC and CCFC curves were used to model the stability constants from the DCP experimental data. In figure 3(A), ECFC for $[L_T]:[Pb_T] = 198$, $[Pb^{2+}] = 3 \times 10^{-5}$ M (open squares), is represented and compared with CCFC for $Pb_x(OH)_y$ species alone. For pH values higher than 6, the gap between these two curves with a maximum value of 88 mV shows complexation between Pb and DIPSO. Furthermore, the CCFC of the $Pb_x(OH)_y$ species predicts precipitation at pH 7.8, which was not observed experimentally. For the two proposed models, the refined stability constants are presented in table 2. The $\log \beta$ values obtained for $PbL(OH)$ (10.33) and $PbL(OH)_2$ (15.71) are significantly larger than the ones predicted theoretically: $\log \beta_{PbL(OH)} = \log \beta_{PbL} + \log \beta_{Pb(OH)} = 3.49 + 5.9 = 9.39$ and $\log \beta_{PbL(OH)_2} = \log \beta_{PbL} + \log \beta_{PbL(OH)_2} = 3.11 + 10.4 = 13.89$. The stability constants, refined for model II, were 12.66 for $PbL_2(OH)$ and 17.98 for $PbL_2(OH)_2$, while the

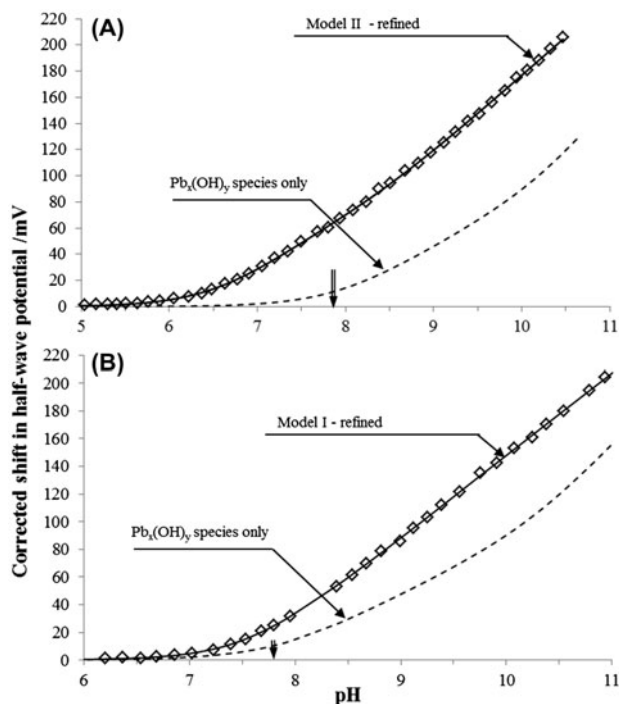


Figure 3. Experimental (open squares, DCP data) and calculated (lines) complex formation curves for the (A) Pb-(DIPSO) $_x$ -(OH) $_y$ and (B) Pb-(AMPSO) $_x$ -(OH) $_y$ systems. (A) $[L_T]:[Pb_T]$ ratio 198, $[Pb_T] = 3.0 \times 10^{-5}$ M. (B) $[L_T]:[Pb_T]$ ratio 490, $[Pb_T] = 4.0 \times 10^{-5}$ M. Vertical double arrow indicates precipitation of $Pb(OH)_2$ in the absence of ligand complexation.

Table 2. Stability constants (as $\log \beta$ values) for the $\text{Pb}-(\text{DIPSO})_x-(\text{OH})_y$ system determined at 25 °C and $\mu = 0.1$ M by DCP and GEP.

Ligand	DIPSO			
	DCP		GEP	
Technique	198		6.3	
$[\text{L}^-]/[\text{Pb}^{2+}]$	3.0×10^{-5}		9.65×10^{-4}	
$[\text{Pb}^{2+}]$ (M)	1.9×10^{-5}		9.65×10^{-4}	
Complexes	Model I	Model II	Model I	Model II
PbL	3.49 ± 0.03	3.48 ± 0.04	3.360 ± 0.006	3.402 ± 0.006
PbL(OH)	10.33 ± 0.02	NI	10.459 ± 0.005	NI
PbL(OH) ₂	15.71 ± 0.01	NI	16.12 ± 0.01	NI
PbL ₂	NI	6.45 ± 0.06	NI	6.347 ± 0.009
PbL ₂ (OH)	NI	12.66 ± 0.03	NI	13.020 ± 0.007
PbL ₂ (OH) ₂	NI	17.98 ± 0.01	NI	18.33 ± 0.01
SD (mV)	0.68	0.68	—	—
Hamilton <i>R</i> -factor	—	—	0.017	0.015
Number of points	52	79	332^a	609^a
pH range	$3.0-10.5$	$3.4-11.0$	$4.5-8.0$	$3.6-9.0$

Notes: NI – not included.

^aNumber of points resulted from the simultaneous refinement of two titrations.

theoretical values are $\log \beta_{\text{PbL}_2(\text{OH})} = \log \beta_{\text{PbL}_2} + \log \beta_{\text{Pb}(\text{OH})} = 6.51 + 5.9 = 12.35$ and $\log \beta_{\text{PbL}_2(\text{OH})_2} = \log \beta_{\text{PbL}_2} + \log \beta_{\text{Pb}(\text{OH})_2} = 6.51 + 10.4 = 16.85$. This analysis shows that the refined stability constant for $\text{PbL}_2(\text{OH})$ is close to what was expected from hydrolysis, while $\text{PbL}_2(\text{OH})_2$ is a little bit higher. For model I, the refined values of $\text{PbL}(\text{OH})_y$, especially $\text{PbL}(\text{OH})_2$, are much larger than the theoretical ones, indicating that model II might be more appropriate.

In order to have further evidence for the model that describes the complexation between Pb and DIPSO better, GEP experiments were designed. With the purpose of choosing the best conditions for the GEP experiments, speciation distribution diagrams were simulated for different $[\text{L}_\text{T}]:[\text{Pb}_\text{T}]$ ratios using the stability constants obtained by DCP. For lower $[\text{L}_\text{T}]:[\text{Pb}_\text{T}]$ ratios, precipitation was predicted at pH below 8, which would not allow accurate refinement of the stability constants of $\text{PbL}_2(\text{OH})_2$. By increasing the $[\text{L}_\text{T}]:[\text{Pb}_\text{T}]$ ratio to 6, precipitation of $\text{Pb}(\text{OH})_2$ is predicted at pH 8.2 and, for a ratio of 10, no precipitation is predicted, which allows a more complete study of the complexation. Therefore, independent titrations were run using these two experimental conditions (table 2). The stability constants refined from GEP results did not differ significantly from the ones obtained by DCP experiments. In addition, the analysis of the Hamilton R-factor indicates a very good fit. To analyze the adjusted model and compare with the experimental data, complex-formation values, Z_M [29], were calculated and are presented in figure 4 as a function of $-\log[\text{L}]$ (as an example, results of only one titration are plotted in the figure). Z_M function increased until 2.0, which suggests the presence of the PbL_2 ; then, it starts to curve back, a typical behavior of systems where hydrolysis of the complexes takes place, to form $\text{PbL}_2(\text{OH})_y$ species. Even though the Hamilton R-factor obtained for model I is low, indicating good agreement between the observed and calculated data, it is possible to observe that the curve based on the refined stability constants is not completely adjusted to the experimental points, especially in the pH range 7.0–7.8, which corresponds to the pL range 3.0–2.8

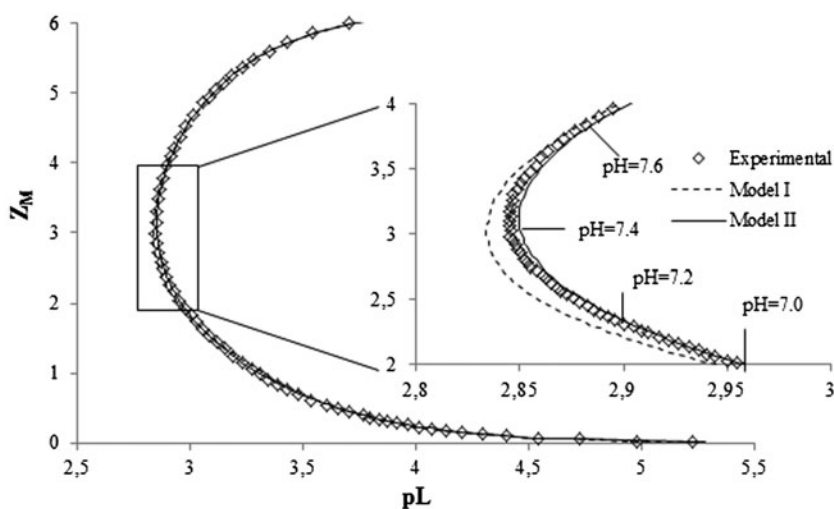


Figure 4. Z_M function for the Pb-AMPSO system. The refined models and experimental conditions are described in table 3.

(see insert in the figure). On the other hand, the calculated curve for model II adjusts perfectly to the observed data and clearly indicates that model II should be the correct one.

From all refined stability constant values (DCP and GEP), the stability constants (as $\log \beta$) for the final model of $\text{Pb}-(\text{DIPSO})_x-(\text{OH})_y$ system were defined as: $\text{PbL} = 3.4 \pm 0.1$, $\text{PbL}_2 = 6.35 \pm 0.15$, $\text{PbL}_2(\text{OH}) = 12.8 \pm 0.2$, and $\text{PbL}_2(\text{OH})_2 = 18.0 \pm 0.3$. To test the proposed final model, species distribution diagrams were generated for $[\text{L}_T]:[\text{Pb}_T]$ ratio of 198 and 6.3 (figure 5), the experimental conditions used for DCP and GEP, respectively. The formation of the species predicted by species distribution diagrams do not differ significantly for both $[\text{L}_T]:[\text{Pb}_T]$ ratios. At pH 6.3, formation of 40% PbL is predicted, while a maximum amount (38 and 42% for 6.3 and 198 $[\text{L}_T]:[\text{Pb}_T]$ ratios, respectively) of PbL_2 occurs at pH 7.0, in conformity with the recorded Z_M value (at pL value of 2.95, corresponding to pH 7.0, Z_M value is 2; see insert in figure 4) and the slope observed in $E_{1/2}$ vs $\log[\text{L}]$ graphic (in the pL range between 3 and 2.6, which corresponds to a pH range between 6.9 and 7.5, a slope of 60.9, typical of the formation of PbL_2 , is observed (figure 2(B)). For pH values above the pK_a , the main species are hydrolyzed forms of the PbL_2 , $\text{PbL}_2(\text{OH})$ and $\text{PbL}_2(\text{OH})_2$; these species are strong enough to avoid formation of several lead hydroxides as well as precipitation of $\text{Pb}(\text{OH})_2$ mainly for higher $[\text{L}_T]:[\text{Pb}_T]$ ratios. In the pH range between 7.4 and 8.6, figure 5(A) shows formation of $\text{PbL}_2(\text{OH})$, as a major species, together with smaller amounts of PbL_2 and $\text{PbL}_2(\text{OH})_2$. These results are

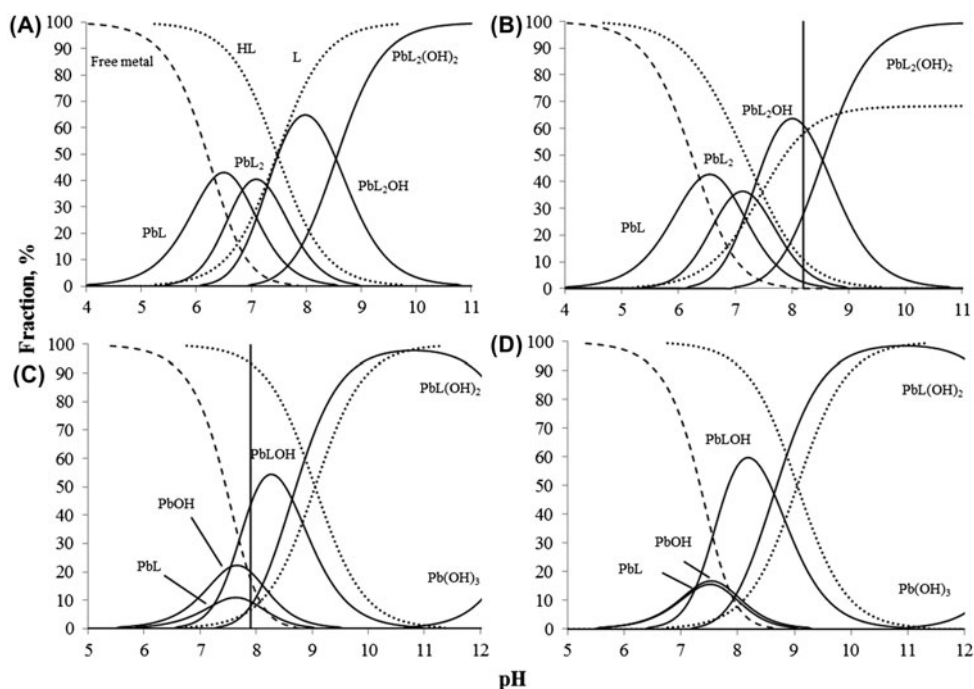


Figure 5. Species distribution diagrams computed for (A, B) $\text{Pb}-(\text{DIPSO})_x(\text{OH})_y$ and (C, D) $\text{Pb}-(\text{AMPSO})_x(\text{OH})_y$ systems. (A) $[\text{L}_T]:[\text{Pb}_T] = 198$, $[\text{Pb}_T] = 3.0 \times 10^{-5}$ M; (B) $[\text{L}_T]:[\text{Pb}_T] = 6.3$, $[\text{Pb}_T] = 9.7 \times 10^{-4}$ M; (C) $[\text{L}_T]:[\text{Pb}_T] = 205$, $[\text{Pb}_T] = 5.1 \times 10^{-5}$ M; (D) $[\text{L}_T]:[\text{Pb}_T] = 490$, $[\text{Pb}_T] = 4.0 \times 10^{-5}$ M. For $\text{Pb}-(\text{DIPSO})_x(\text{OH})_y$ system, the metal-ligand model consisted of PbL , PbL_2 , $\text{PbL}_2(\text{OH})$, and $\text{PbL}_2(\text{OH})_2$ for which stability constants, as $\log \beta$, were set to 3.4, 6.35, 12.8 and 18.0, respectively. For $\text{Pb}-(\text{AMPSO})_x(\text{OH})_y$ system, the metal-ligand model consisted of PbL , $\text{PbL}(\text{OH})$, and $\text{PbL}(\text{OH})_2$ for which stability constants, as $\log \beta$, were set to 2.9, 9.4 and 14.5, respectively.

in agreement with the slope of 44 mV/pH recorded in this range of pH (figure 2(A)), which results from a weighted average of slope values due to the mixed species present, as discussed previously. Above pH 8.6, $\text{PbL}_2(\text{OH})_2$ species are formed as a major species, consistent with a slope of 59 mV/pH (figure 2(A)) recorded in this pH range. Additionally, for a $[\text{L}_T]:[\text{Pb}_T]$ ratio of 6.3, figure 5(B) shows that above pH 6.3 and up to precipitation, there is simultaneous formation of PbL_2 and $\text{PbL}_2(\text{OH})$, which explains the back fanning behavior of Z_M in this range of pH (see insert in figure 4).

3.2.2. Pb-AMPSO system. First, one DCP experiment using a similar $[\text{L}_T]:[\text{Pb}_T]$ ratio to the ones used for the Pb-DIPSO system was performed: $[\text{L}_T]:[\text{Pb}_T]$ ratio at 205 with $[\text{Pb}_T] = 5.1 \times 10^{-5}$ M. Under these conditions, an abrupt decrease in the recorded current (in a very narrow pH range) (figure 6) was observed that could not be explained in terms of the formation of a complex in such a narrow pH range. This decrease could be rationalized in terms of precipitation of $\text{Pb}(\text{OH})_2$ and this was experimentally verified. From this result, it becomes clear that much higher $[\text{L}_T]:[\text{Pb}_T]$ ratios than those used for the Pb-DIPSO system should be used for full characterization of the Pb-AMPSO system in the pH range (pH between 8 and 10), where AMPSO can be used as a buffer.

So, additional independent DCP experiments were performed at $[\text{L}_T]:[\text{Pb}_T]$ ratio 490 (two experiments), 450 and 402, all with $[\text{Pb}_T] = 4.0 \times 10^{-5}$ M. For all cases, no precipitation was observed in the titrations. Results and discussion of the graphical analysis of $E_{1/2}$ vs. pH function are presented for $[\text{L}_T]:[\text{Pb}_T] = 490$, $[\text{Pb}_T] = 4.0 \times 10^{-5}$ M (figure 2(C)). The variation of the half-wave potential as a function of pH does not indicate significant complexation up to pH 7. For higher pH, complexation is observed and three regions can be distinguished. Between pH 7.1 and 7.9, the experimental slope is very close to the theoretical Nernst slope for electrochemical reactions involving one proton, 29 mV/pH. At this pH range, the ligand is mainly in the protonated form, as the pH is below the $\text{p}K_a$; thus, this slope can indicate reduction of PbL according to equation (2). The formation of the hydroxocomplex PbOH^+ also meets the criteria of one proton reaction (equation (3)). When the pH of the solution is above 8, a slope of about 60 mV/pH can be identified

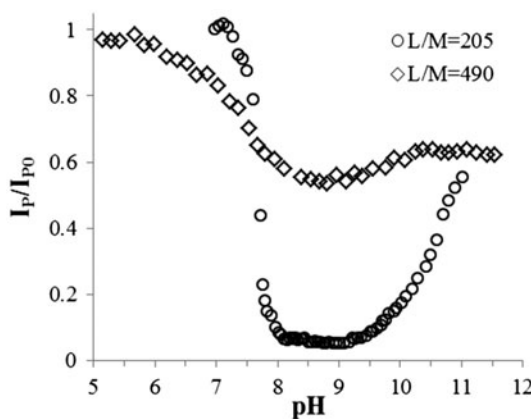
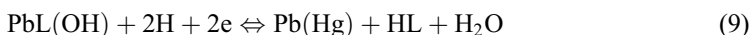


Figure 6. Variation in the normalized diffusion current, calculated from DCP waves, throughout the polarographic titrations of $\text{Pb}-(\text{AMPSO})_x(\text{OH})_y$ system.

(figure 2(C)). Between pH 8 and 9, the protonated form of the ligand, HL, is the main species present in solution but some deprotonated L^- already exists. If two protons were involved in the reaction, a theoretical slope of 59 mV/pH should be expected. This slope indicates that PbL_2 and/or $PbL(OH)$ will predominate in this pH range according to equations (7) and (9), respectively:



With increasing pH, the ligand is mainly deprotonated and the formation of $PbL_x(OH)_2$ species may explain the slope observed for pH higher than 9, as two protons are involved in the reaction (equation (5)). The formation of lead hydroxide, $Pb(OH)_2$, is unlikely since no precipitation was observed.

When the half-wave potential is represented as a function of $\log[L]$ (figure 2(D)), a slope of -30 mV/ $\log[L]$ can be drawn between $\log[L]$ -3.5 and -3.1 (pH 7.3–7.8), which is very close to the theoretical slope for the electrochemical reaction involving one ligand, additional evidence that PbL is formed in this pH range. A slope close to -59 mV/ $\log[L]$ can also be drawn, between the points corresponding to the pH range 8.0–8.6. For $[L_T]:[Pb_T] = 402$ and 450, similar slope profiles to that recorded for $[L_T]:[Pb_T] = 490$ were obtained (data not shown).

According to the graphical analysis performed above, the following two models should be considered:

- (I) $PbL, PbL(OH), PbL(OH)_2$
- (II) $PbL, PbL_2, PbL_2(OH), PbL_2(OH)_2$

As one can observe in table 3, good fits are achieved for both models for $[L_T]:[Pb_T]$ ratio 490, $[Pb_T] 4.0 \times 10^{-5}$ M; similar results are obtained for the other $[L_T]:[Pb_T]$ ratios (data not shown). Assuming that, $PbL_x(OH)$ and $PbL_x(OH)_2$ complexes are formed from the hydrolysis of PbL_x complexes, it is possible to compare the refined stability constants for such complexes

Table 3. Stability constants (as $\log \beta$ values) for the $Pb-(AMPSO)_x-(OH)_y$.

Ligand	AMPSO					
	DCP					
Technique						
$[L_T]/[Pb_T]$	490		490		402	450
$[Pb_T]$ (M)	4×10^{-5}		4×10^{-5}		4×10^{-5}	4×10^{-5}
Complexes	Model I	Model II	Model III	Model I	Model I	Model I
PbL	3.11 ± 0.07	3.1 ± 0.1	NI	2.6 ± 0.2	3.38 ± 0.04	3.26 ± 0.07
PbL(OH)	9.45 ± 0.03	NI	9.55 ± 0.02	9.30 ± 0.04	9.50 ± 0.02	9.46 ± 0.03
PbL(OH) ₂	14.26 ± 0.01	NI	14.24 ± 0.01	14.47 ± 0.02	14.50 ± 0.01	14.68 ± 0.01
PbL ₂	NI	6.51 ± 0.05	NI	NI	NI	NI
PbL ₂ (OH)	NI	11.53 ± 0.05	NI	NI	NI	NI
PbL ₂ (OH) ₂	NI	16.04 ± 0.01	NI	NI	NI	NI
SD (mV)	0.48	0.46	1.36	0.42	0.97	2.62
Number of points		43		33	48	36
pH range		4.0–11.5		3.5–10.8	3.4–11.8	3.4–10.0

Note: System determined at 25 °C and $\mu = 0.1$ M by DCP.

with the theoretical values. For $[L_T]:[Pb_T] = 490$, the $\log \beta$ values obtained for $PbL(OH)$ (9.45) and $PbL(OH)_2$ (14.26) are slightly larger than the ones predicted theoretically: $\log \beta_{PbL(OH)} = \log \beta_{PbL} + \log \beta_{Pb(OH)} = 3.11 + 5.9 = 9.01$ and $\log \beta_{PbL(OH)_2} = \log \beta_{PbL} + \log \beta_{Pb(OH)_2} = 3.11 + 10.4 = 13.51$. The stability constants, refined for model II, were 11.53 for $PbL_2(OH)$ and 16.04 for $PbL_2(OH)_2$, while theoretical values are $\log \beta_{PbL_2(OH)} = \log \beta_{PbL_2} + \log \beta_{Pb(OH)} = 6.51 + 5.9 = 12.41$ and $\log \beta_{PbL_2(OH)_2} = \log \beta_{PbL_2} + \log \beta_{Pb(OH)_2} = 6.51 + 10.4 = 16.91$. This comparative analysis shows that the value of the refined stability constant for $PbL(OH)$ was almost as expected from hydrolysis, whereas for $PbL(OH)_2$ it is a little bit higher. For model II, the refined values of $PbL_2(OH)$ and $PbL_2(OH)_2$ are much lower than the theoretical ones. Additionally, the refined $\log \beta_{PbL}$ was 3.11 ± 0.07 , while the refined $\log \beta_{PbL_2}$ was 6.51 ± 0.05 . If the value of the stability constant for PbL is 3.1, then the expected value for PbL_2 should not be higher than 6.2 (twice the $\log \beta_{PbL}$). These results explain why theoretical values calculated for $PbL_2(OH)$ and $PbL_2(OH)_2$ are much higher than the refined ones and suggest that model I should be the correct one.

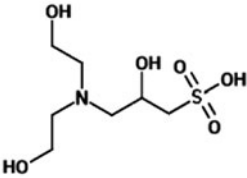
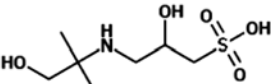
For all $[L_T]:[Pb_T]$ ratios, the refined $\log \beta_{PbL}$ was 2.9 ± 0.5 (note that the standard deviation represents here the ranges in the stability constant value obtained from all $[L_T]:[Pb_T]$ ratios). This is a somewhat higher standard deviation than is usually found. In order to clarify this point, another model (model III; only for $[L_T]:[Pb_T] = 490$), where PbL was not taken into account, was refined (table 3). The refined stability constant values for $PbL(OH)$ and $PbL(OH)_2$ species did not differ significantly from the ones obtained for model I, which suggests that $PbL(OH)$ and $PbL(OH)_2$ species are the major ones. However, the overall standard deviation (SD) value is much higher than the one obtained when model I was refined (table 3). Thus, it appears that PbL is formed since a best fitting (lower SD) is obtained when PbL is included in model I. Moreover, the difference between the ECFC for $[L_T]:[Pb_T] = 490$, $[Pb_T] = 4.0 \times 10^{-5}$ M and the CCFC generated for $Pb_x(OH)_y$ species (figure 3(B) observed in the pH range 7.2–8, clearly shows that PbL is formed and corroborates the experimental slope of -28 mV/ $\log[L]$ drawn in figure 2(D). From this analysis, we conclude that model I describes quite well the experimental results.

To test if it could be possible to confirm the proposed model from results obtained by GEP experiments, the stability constants obtained by DCP were used to generate species distribution diagrams for different $[L_T]:[Pb_T]$ ratios. Typical experiments using GEP require much lower ratios and higher $[Pb_T]$ than DCP. For example, considering a $[L_T]:[Pb_T] = 20$, $[Pb_T] = 5.0 \times 10^{-4}$ M, already a very extreme situation to be studied with GEP due to a high ratio of $[L^-]/[\sum_{x,y=0}^2 PbL_x(OH)_y^{(2-x-y)}]$, which leads to erroneous stability constants [30], precipitation of $Pb(OH)_2$ is predicted at pH 7.8 (data not shown); up to this pH, species distribution diagram shows that formation of Pb -AMPSO complexes is not predicted in significant quantities to be refined: maximum of 10% of PbL and no formation of $PbL_x(OH)$ species. Thus, GEP experiments are not suitable for characterization of the Pb -AMPSO $_x$ -(OH) $_y$ system.

From all refined stability constants values obtained from all $[L_T]:[Pb_T]$ ratios (table 3), the stability constants (as $\log \beta$) for the Pb -AMPSO $_x$ -(OH) $_y$ system were defined as $PbL = 2.9 \pm 0.5$, $PbL(OH) = 9.4 \pm 0.1$ and $PbL(OH)_2 = 14.5 \pm 0.2$.

Using the final model, species distribution diagrams were generated for $[L_T]:[Pb_T]$ ratios 205 ($[Pb^{2+}] = 5.1 \times 10^{-5}$ M) and 490 ($[Pb_T] = 4.0 \times 10^{-5}$ M) and plotted in figure 5(C) and (D). Figure 5(C) predicts precipitation of $Pb(OH)_2$ at pH 7.6 and this was experimentally verified (see the abrupt decrease of the current in figure 6, which is clear evidence of precipitation). On the other hand, for $[L_T]:[Pb_T]$ ratios 490 (figure 5(D)) no precipitation of $Pb(OH)_2$ is foreseen, which is in perfect agreement with our experimental results. For pH

Table 4. Proposed final model for the $\text{Pb}-(\text{DIPSO})_x-(\text{OH})_y$ and $\text{Pb}-(\text{AMPSO})_x-(\text{OH})_y$ systems and comparison with ammonia.

Ligand	NH_3	DIPSO	AMPSO
Structure			
$\text{p}K_a$	9.26	7.47	9.05
$\text{Log } \beta$			
PbL	1.55	3.4 ± 0.1	2.9 ± 0.5
PbL(OH)	–	–	9.4 ± 0.1
PbL(OH) ₂	–	–	14.5 ± 0.2
PbL ₂	–	6.35 ± 0.35	–
PbL ₂ (OH)	–	12.8 ± 0.2	–
PbL ₂ (OH) ₂	–	18.0 ± 0.3	–
References	[24]	[18]	[25]

values higher than 6, figure 5(D) indicates that PbL and Pb(OH) start to be formed concomitantly and a maximum amount of these two species is observed between pH 7 and 8; this observation correlates well with the slopes of about 29 mV/pH (figure 2(C) and (D) drawn in this pH range. The simultaneous formation of PbL and Pb(OH) explain the high variability of the stability constant values refined for PbL (table 3). For pH values higher than 7, PbL(OH) starts to be formed and is a major species in the pH range between 7.7 and 8.7, which seems to correlate well with the experimental slope of about 59 mV/pH (figure 2(C)) drawn in this pH range. In this pH range, the ligand is mainly protonated but a small amount exists in the deprotonated form, which would generate an experimental slope lower than 59 mV/pH. However, the species distribution diagram also shows that PbL(OH)₂ starts to be formed at pH 7.5, which explains why the experimental slope gets a value of 59 mV/pH in this pH range, as well as for higher pH values (figure 2(C)).

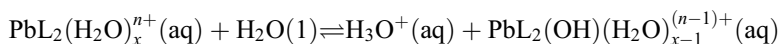
4. Final analysis of the models and stability constants of $\text{Pb}-(\text{Ligand})_x-(\text{OH})_y$ systems

DIPSO and AMPSO are zwitterionic buffers, with structures, protonation constants and overall lead stability constants of the final models compiled in table 4, together with values for ammonia. A comparative analysis between the $\text{log } \beta_{\text{PbL}}$ for both $\text{Pb}-(\text{Ligand})_x-(\text{OH})_y$ systems, studied in this work, and ammonia clearly suggests that both ligands do not act as monodentate. Probably, DIPSO acts as a tridentate ligand coordinating through the amino and two hydroxyl groups, forming two five-member chelate rings. On the other hand, AMPSO behaves most likely as a bidentate ligand coordinating via amino and β -hydroxyl groups near the sulfonic group forming one five-member chelate ring. A similar behavior was also verified for $\text{log } \beta_{\text{CdL}}$ for $\text{Cd}-(\text{DIPSO})_x-(\text{OH})_y$ and $\text{Cd}-(\text{AMPSO})_x-(\text{OH})_y$ systems [16, 17].

Even though, DIPSO and AMPSO have related structures (table 4), the final proposed models for both $\text{Pb}-(\text{Ligand})_x-(\text{OH})_y$ systems are different, probably due to the fact that AMPSO is much more basic than DIPSO (table 4), and starts to deprotonate more than one log unit higher than DIPSO (figure 5). This behavior, together with the fact that these two ligands complex lead in the pH region, where lead hydrolysis is very significant, mainly for

AMPSO (see figure 3(B)), explains why for the $\text{Pb}-(\text{AMPSO})_x-(\text{OH})_y$ system, $\text{PbL}(\text{OH})$ is formed instead of PbL_2 .

Some amino alcohol complexes of copper (II) and nickel(II) undergo deprotonation of the coordinated hydroxyl groups in neutral or basic media, simultaneously resulting in formation of a bond between the metal and the negatively charged alkoxide oxygen [31]. In the present study, neither GEP nor DCP can distinguish between $[\text{Pb}(\text{L})_x\text{H}_{-y}]$ or $[\text{Pb}(\text{L})_x(\text{OH})_y]$ complexes. However, as far as we know, no further information about the structure of the complexes can be obtained; under the experimental conditions used in this work, the complexes are totally soluble, which does not allow collecting the solid and characterizing it by other solid-state techniques, such as X-ray diffraction. On the other hand, DIPSO and especially AMPSO are very basic ligands and form complexes with lead in the pH range where hydrolysis of lead occurs. Thus, very high $[\text{L}_\text{T}]:[\text{Pb}_\text{T}]$ ratios using very low lead concentration (for further details see tables 2 and 3) were necessary to be used to characterize properly the systems in the buffering pH range, where these buffers are active. Thus, DCP was the only technique that fulfilled these conditions for both $\text{Pb}-(\text{Ligand})_x-(\text{OH})_y$ systems. So, according to the final model described for the Pb-DIPSO system, the refined stability constant for $\text{PbL}_2(\text{OH})$ species suggests that formation of this species resulted from hydrolysis of PbL_2 according to the following reaction:



Since the value of the stability constant of $\text{Pb}_2\text{L}(\text{OH})$ (12.8) is just the sum of: $\log \beta_{\text{PbL}_2} + \log \beta_{\text{Pb}(\text{OH})} = \log \beta_{\text{PbL}_2(\text{OH})} = 6.35 + 5.9 = 12.25$. On the other hand, the refined stability constant for $\text{PbL}_2(\text{OH})_2$ (18.0) is much higher than the value predicted theoretically (16.75) from the hydrolysis of PbL_2 , which can be an indication that $\text{Pb}(\text{L})\text{H}_{-1}$ is formed. According to the accepted model for the Pb-AMPSO system, the comparison between the refined stability constant values for $\text{PbL}(\text{OH})$ and $\text{PbL}(\text{OH})_2$ species, which are $\log \beta_{\text{PbL}(\text{OH})} = 9.4$ and $\log \beta_{\text{PbL}(\text{OH})_2} = 14.5$, respectively, and those predicted theoretically assuming the hydrolysis of PbL [$\log \beta_{\text{PbL}(\text{OH})} = \log \beta_{\text{PbL}} + \log \beta_{\text{Pb}(\text{OH})} = 2.9 + 5.9 = 8.88$ and $\log \beta_{\text{PbL}(\text{OH})_2} = \log \beta_{\text{PbL}} + \log \beta_{\text{Pb}(\text{OH})_2} = 2.9 + 10.4 = 13.3$] suggests that formation of $\text{PbL}(\text{OH})$ resulted from hydrolysis of PbL , whereas the second species results from ionization of the OH groups of AMPSO and thus should probably be $[\text{Pb}(\text{L})\text{H}_{-2}]$.

Acknowledgments

The authors thank Professor Ignacy Cukrowski from the University of Pretoria (South Africa) for polarographic modeling software (3D-CFC program) and Professor Carlos Gomes from the Faculty of Sciences/Porto University for the COPOTISY program.

Funding

This work has been supported by Fundação para a Ciência e a Tecnologia (FCT), from the Portuguese Government, through [grant number PEst-C/EQB/LA0006/2011]; Isabel Pinto and Georgina Alves acknowledge their grant scholarships [SFRH/BD/70450/2010 and SFRH/BD/46521/2008, respectively] financed by FCT.

References

- [1] N.E. Good, G.D. Winget, W. Winter, T.N. Connolly, S. Izawa, R.M.M. Singh. *Biochemistry*, **5**, 467 (1966).
- [2] O.M. Lage, M.T.S.D. Vasconcelos, H.M.V.M. Soares, J.M. Osswald, F. Sansonetty, A.M. Parente, R. Salema. *Arch. Environ. Contam. Toxicol.*, **31**, 199 (1996).
- [3] S.M. Downs, A.M. Mastropolo. *Mol. Reprod. Dev.*, **46**, 551 (1997).
- [4] J.E. Swain, T.B. Pool. *Reprod. Biomed. Online*, **18**, 799 (2009).
- [5] M.A. Sharpe, J.M. Wigglesworth, J. Loewen, P. Nicholls. *Biochem. Biophys. Res. Commun.*, **216**, 931 (1995).
- [6] M. Kreiner, M.C. Parker. *Biotechnol. Bioeng.*, **87**, 24 (2004).
- [7] D.P. McGregor, S. Forster, J. Steven, J. Adair, S.E.C. Leary, D.L. Leslie, W.J. Harris, R.W. Titball. *Biotechniques*, **21**, 463 (1996).
- [8] T. Arai, N. Nimura, T. Kinoshita. *Biomed. Chromatogr.*, **9**, 68 (1995).
- [9] I.E. Valko, H. Siren, M.L. Riekkola, J.H. Jumppanen. *J. Microcolumn Sep.*, **8**, 421 (1996).
- [10] S.K. Wiedmer, J.H. Jumppanen, H. Haario, M.L. Riekkola. *Electrophoresis*, **17**, 1931 (1996).
- [11] M. Hosse, K.J. Wilkinson. *Environ. Sci. Technol.*, **35**, 4301 (2001).
- [12] M.T.S.D. Vasconcelos, M.A.G.O. Azenha, C.M.R. Almeida. *Anal. Biochem.*, **265**, 193 (1998).
- [13] D.L. Vullo, H.M. Ceretti, M. Alejandra Daniel, S.A.M. Ramirez, A. Zalts. *Bioresour. Technol.*, **99**, 5574 (2008).
- [14] C.M.M. Machado, I. Cukrowski, H. Soares. *Helv. Chim. Acta*, **86**, 3288 (2003).
- [15] C.M.M. Machado, S. Scheerlinck, I. Cukrowski, H.M.V.M. Soares. *Anal. Chim. Acta*, **518**, 117 (2004).
- [16] C.M.M. Machado, I. Cukrowski, H. Soares. *Electroanalysis*, **18**, 719 (2006).
- [17] C.M.M. Machado, G.M.S. Alves, I.S.S. Pinto, S. Van Acker, H.M.V.M. Soares. *J. Sol. Chem* **42**, 1602 (2013).
- [18] C.M.M. Machado, I. Cukrowski, P. Gameiro, H.M.V.M. Soares. *Anal. Chim. Acta*, **493**, 105 (2003).
- [19] A.J. Bard, L. Faulkner. *Electrochemical Methods – Fundamentals and Applications*, Wiley, New York (1980).
- [20] I. Cukrowski. *Anal. Chim. Acta*, **336**, 23 (1996).
- [21] I. Cukrowski, M. Adsetts. *J. Electroanal. Chem.*, **429**, 129 (1997).
- [22] P.M. May, K. Murray, D.R. Williams. *Talanta*, **32**, 483 (1985).
- [23] P.M. May, K. Murray, D.R. Williams. *Talanta*, **35**, 825 (1988).
- [24] R.M. Smith, A.E. Martell. *NIST Standard Reference Database 46, NIST Critically Selected Stability Constants of Metal Complexes Database (Version 3.0)*, US Department of Commerce, National Institute of Standards and Technology (1997).
- [25] H.A. Azab, A.S. Orabi, E.T.A. El-Salam. *J. Chem. Eng. Data*, **46**, 346 (2001).
- [26] K.J. Powell, P.L. Brown, R.H. Byrne, T. Gajda, G. Hefter, A.K. Leuz, S. Sjoberg, H. Wanner. *Pure Appl. Chem.*, **81**, 2425 (2009).
- [27] M.B. Shchigol. *Zhurnal Neorganicheskoi Khimii*, **8**, 1361 (1963).
- [28] D.R. Crow. *Polarography of Metal Complexes*, Academic Press, London (1969).
- [29] F. Marsicano, C. Monberg, B.S. Martincigh, K. Murray, P.M. May, D.R. Williams. *J. Coord. Chem.*, **16**, 321 (1988).
- [30] C.M.M. Machado, H.M.V.M. Soares. *Talanta*, **71**, 1352 (2007).
- [31] K.H. Hong, K.S. Bai. *Bull. Korean Chem. Soc.*, **19**, 197 (1998).